Journal of Building Engineering 105 (2025) 112531

Contents lists available at ScienceDirect

Journal of Building Engineering

journal homepage: www.elsevier.com/locate/jobe

Experimental investigation on the performance of ground granulated blast furnace slag and copper slag blended recycled aggregate concrete exposed to elevated temperatures

Anasuya Sahu [a,*], Sanjay Kumar [a], Adarsh Srivastav [b], Harsh Anurag [b]

[a] Department of Civil Engineering, National Institute of Technology, Jamshedpur, 831014, Jharkhand, India
[b] Department of Civil Engineering, Indian Institute of Technology, BHU, India

ARTICLE INFO

Keywords:
Recycled concrete aggregate
Copper slag
Ground granulated blast furnace slag
Mechanical properties
Elevated temperature

ABSTRACT

The current experimental programme examines the residual performance of recycled aggregate concrete (RAC) under elevated temperatures, with partial replacement of fine aggregate by copper slag, followed by the substitution of cement with ground granulated blast furnace slag (GGBFS). RAC was prepared by replacing natural coarse aggregate with recycled coarse aggregate (RCA) at substitution levels of 0 %, 33 %, 66 %, and 100 %. Among these, the 33 % RCA replacement demonstrated superior mechanical properties and was selected for further investigation. Subsequently, the industrial wastes like copper slag and GGBFS were used for replacing fine aggregate and cement up to 60 % to escalate the residual characteristics of RAC mixes prepared with 33 % RCA. All the specimens were exposed at temperature level of 30 °C, 200 °C, 400 °C, 600 °C and 800 °C respectively and assessed their residual compressive strength, split tensile strength, elastic modulus, and failure behavior by conducting laboratory experiments. Test results concluded that, the GGBFS and CS blended RAC mixture achieved greater resistance to deterioration of strength properties compared to the control mixture at higher temperature. The combination of 33 % RCA, 40 % CS, and 40 % GGBFS exhibited superior residual performance over all the mixes and established grater fire-resistant to concrete. Further, the microstructural study of different RAC mixtures revealed that the addition of CS and GGBFS strengthened the RAC matrix by creating a dense calcium silicate hydrate gel.

1. Introduction

Over the past decade, the extensive use of natural materials in concrete production driven by rapid industrialization and urbanization has posed significant environmental challenges. The global annual concrete production is estimated to be approximately 25 billion tonnes [1]. Similarly, the demand for building aggregates, a key component of concrete is projected to increase to 80 billion tonnes worldwide by 2032 (PMR, 2023). Meanwhile, the generation of vast amounts of waste from the construction and industrial sectors has heightened the environmental pollution and exacerbated disposal challenges. In this context, recycling and repurposing waste materials offer a viable solution to reduce the consumption of natural resources in construction while addressing environmental and waste disposal concerns. From this perspective, recycled coarse aggregate (RCA), derived from construction and demolition waste,

* Corresponding author. Department of Civil Engineering, National Institute of Technology, Jamshedpur, Jharkhand, India.
E-mail address: 2020rsce007@nitjsr.ac.in (A. Sahu).

https://doi.org/10.1016/j.jobe.2025.112531
Received 18 January 2025; Received in revised form 22 March 2025; Accepted 31 March 2025
Available online 1 April 2025

along with copper slag (CS) and GGBFS, by-products of copper and iron industries, represent promising sustainable alternatives to virgin construction materials. In the present study, RCA replaced the natural coarse aggregate (NCA) entirely (up to 100 %), while copper slag and GGBFS were incorporated as substitutes for natural fine aggregate (NFA) and cement, respectively, at levels up to 60 %, to produce environmentally friendly and sustainable concrete. RCA, obtained through proper recycling and sieving processes, is widely utilized as a substitute for NCA due to its favourable properties. Studies have shown that replacing NCA with RCA at levels up to 30 % enhances the physical and mechanical properties of concrete [2–10]. However, beyond 30 %, the performance deteriorates due to the increased presence of adhered cement mortar on the RCA surface, which adversely affects its quality [11–18]. According to Patra et al. [19], the mechanical performance of RAC was reduced up to 50 % after replacing NCA with RCA up to 60 %. Furthermore, the high mass loss in RAC at elevated temperature alters its behaviour, increasing porosity and reducing strength [7,20]. In their investigation of the mechanical characteristics of both regular and high strength concrete, Silva et al. [7] substituted RCA for NCA at various ratios and exposing the concrete to temperatures as high as 650 °C. They concluded that RCA substitution had a minimal impact on mechanical performance. According to Salahuddin et al. [9] the residual compressive strength of RAC remained comparable to control concrete though the strength was decreased with the increased temperature of up to 600 °C. Similarly, Sarhat et al. [21] observed that RAC with up to 50 % RCA exhibited superior residual properties compared to conventional concrete.

The manufacturing of primary products and other industrial operations give rise to a variety of by-products that are either completely unusable or barely useful in the industrial sector. Copper slag, fly ash, glass powder, GGBFS, coal bottom ash etc. are some of the industrial wastes which are produced in large volume worldwide in the present decade create a serious challenge to the researchers for their environmental and disposal issue. So, to overcome these situations researchers have put their efforts on recycling of industrial wastes and used as sustainable materials in construction sector. In this context, Copper slag and GGBFS are the most challenging waste materials which are replace the natural materials successfully in sustainable and economic manner. Researchers used Copper slag, a by-product from copper processing industry, as a binder or natural fine aggregate (NFA) due to its better cohesive property, glassy texture, and lower rate of water absorption characteristics [22–25]. Previous research work indicated that CS content in the concrete as a fine aggregate enhanced the workability value [26–29]. Most of the researchers reported that, replacing fine aggregate up to 50 % as CS in concrete improved its mechanical properties [27,29–31]. Similarly, the concrete produced using CS in place of fine aggregate exhibited excellent fire-resistant properties in comparison to normal concrete. The researchers found that the concrete exhibited superior residual mechanical properties by substituting CS in place of fine aggregate up to 40 % at higher temperatures [29,32]. Ameri et al. [29] determined the properties of alkali activated mortar (AAM) at elevated temperature by adding CS from 0 to 100 % as fine aggregate and observed that the AAM with 20 % CS achieved higher strength qualities than the mortar made with NFA at the temperature of 800 °C. Nevertheless, Gong and Ueda [33] found that when the specimens were subjected to 400 °C, the residual compressive strength of self-compacting concrete is reduced when up to 40 % fine aggregate is replaced as a proportion of copper slag. The inconsistent results of these findings highlighted the necessity for more investigation on fire-resistant properties of CS based concrete. Similarly, GGBFS is another industrial waste product from iron industry whose pozzolanic qualities make it a suitable substitute for regular cement as a binder to produce concrete. According to the researcher, the replacement levels of cement with GGBFS were varying from 30 % to 85 % [24]. The compressive strength of concretes containing 30 % GGBFS as a binder was somewhat higher than that of normal concrete [34]. GGBFS as a binder also enhanced the performance of RAC. By adding GGBFS up to 55 % as a binder, Kou et al. [35] examined the mechanical and durability performance of RAC and came to the conclusion that the mechanical strength of RAC was greatly decreased with the addition of large volume GGBFS. In addition, relatively little research has been done to examine the behaviour of RAC combined with GGBFS after high temperature exposure. In contrast, Kou et al. [36] examined and compared the residual strengths of RAC and natural aggregate concrete at elevated temperature by using 55 % GGBFS and 35 % fly ash (FA) as a substitution of binder. The study revealed that, compared to the natural concrete the residual properties of RAC with FA and GGBFS improved up to 300 °C and beyond that significant reduction occurred because of the coarsening of the pore structure. Tung et al. [37] analysed the behaviour of GGBFS blended RAC at elevated temperature by replacing the cement with GGBFS partially at four levels (0 %, 20 %, 40 % and 60 %) and concluded that GGBFS blended RAC exhibited lower rate of degradation of residual mechanical strength in comparison to RAC without GGBFS.

Though the researchers have put their efforts to analyse the residual performance of RAC at high temperature exposures, still it is crucial to evaluate the post fire behaviour of RAC using different waste materials as exposure to fire weakens the strength characteristics of concrete structures. To fill this research gap, current study is concentrated on analysing the residual behaviour of RAC that has been combined with GGBFS and copper slag through various laboratory tests before and after exposed to higher temperature. In their earlier research [38], the authors examined the impact of CS utilising as fine aggregate on the residual performance of RAC and found that, RAC exhibited better fire-resistant properties by substituting CS as a fraction of fine aggregate up to 40 %. So, in the present study authors have put their efforts by substituting GGBFS as binder to replace the cement up to 60 % and studied the performance of CS blended RAC at different temperature exposures. For evaluating mechanical parameters of various concrete mixes, tests for compressive, split tensile strength and modulus of elasticity are performed including varied percentages of RCA, CS, and GGBFS. The tests are conducted at room temperature as well as at increased temperatures up to 800 °C with 200 °C intervals to assess the strength resisting capability and degree of strength degradation in RAC at different temperature exposures. The findings of this investigation enable a clear comparison of control concrete and RAC with and without addition of CS and GGBFS in terms of how their strength degrades in response to high temperature. In addition to this microstructural analysis has been carried out through X-Ray Diffractometer (XRD) and Scanning electron Microscope (SEM) to analyse the different hydrated phases and surface features of concrete samples.

2. Materials used

2.1. Binders

The OPC with 53 grade confirmed from IS: 12269-1987 [39] and GGBFS confirmed to IS: 16714-2018 [40] are used as binder in this study. The GGBFS (Fig. 1) collected from Tata Steel Limited, Jamshedpur is substituted as cement partially. In compliance with the BIS criteria, Table 1 represented the physical characteristics of binders that have been examined in the laboratory. Table 2 displayed the chemical analysis of binders, carried out through X-Ray fluorescence (XRF) test. The surface morphology of cement and GGBFS is displayed in Fig. 2 showing that the particles are distributed around the surface in varying sizes and geometries. It is also observed that the GGBFS particles are relatively more compact and smoother surface as compared to cement particles. This may be due to extensive impact and rubbing of unground blast furnace slag in the ball mill. Fig. 3 shows the grading analysis of OPC and GGBFS performed as per IS:4031(Part 1) and IS:1727. It is observed that GGBFS is finer that OPC which gives early strength to the concrete.

2.2. Aggregates

Present study employed locally available river sand as a natural fine aggregate and crushed granite with a size of 20 mm down as a natural coarse aggregate. Coarse aggregates that have been recycled, as depicted in Fig. 1, are obtained from the demolished old fuel station closed to Jamshedpur with strength grade C35/40. After being properly crushed and sieved, they can be utilized in place of coarse aggregates. The crushing index of RCA is found to be 23.82 % and can be used for concrete work as per guidelines of ACI CRC 18.517 [41]. The aggregate crushing value of RCA and natural coarse aggregate are found to be 22 % and 18.65 % which is determined as per IS:2386 (Part 4) [42] and confirmed to IS: 383 [43] limits. Copper slag (Fig. 1), a waste by-product collected from copper industry is used as fine aggregate. All aggregates have undergone grading analysis in accordance with IS: 2386 (part-I) [44]. Table 1 listed the laboratory test results on physical characteristics of aggregates, whereas Table 2 provides the chemical analysis of NFA and CS. The grading curve for aggregates as shown in Fig. 3 indicated that, the nominal sizes of all the aggregates are satisfied as per IS: 383 [43] limits.

2.3. Admixture

The admixture utilized in this study was PC 200, based on poly-carboxylic ether. The pH of PC 200 is found to be 7.0. The specific gravity is found to be 1.09 with no chloride content.

2.4. Mixing, casting, curing and testing

According to IS:10262 (2019) [45] guidelines, three series of mixes have been developed specifically for M30 grade concrete in this experimental study. In first series, four trial mixes are designed with control mix which is prepared using natural resources and the rest three mixes are made by substituting 33 %, 66 %, and 100 % RCA in place of NCA [38]. The second and third series consists of three trials mixes each that are designed with 33 % RCA by substituting copper slag (20 %, 40 % and 60 %) and GGBFS (20 %, 40 % and 60 %) as fine aggregate and cement respectively. The coarse aggregates utilized in the study are pre-soaked for 24 h before casting to get them to a surface saturated dry condition, which is necessary to produce a workable concrete. The proportions of the design mix for various concrete mixtures were detailed in Table 3. It has been suggested that adding 1 % of the binder's weight in superplasticizer will improve concrete's workability. Three specimens of each concrete mix are mixed, cast, and cured at a temperature of 27 ± 2 °C until they reach maturity. After curing, the specimens are undergone for different tests. The tests are being performed under two

(a) RCA (b) CS (c) GGBFS

Fig. 1. Waste products utilized.

Table 1
Physical characteristics of binders and aggregates.

Material	Appearance	Specific gravity	Density (kg/m^3)	Water absorption (%)	Fineness modulus
OPC	Grey	3.13	1445	–	–
GGBFS	Off-White	2.82	–	–	–
NFA	brown	2.87	1563	1.15	2.4
NCA	Grey	3.2	2664	0.84	5.33
CS	Black	3.5	1952	0.62	3.5
RCA	Light grey	2.7	2376	3.90	5.4

Table 2
Chemical composition of binders and aggregates.

Constituents (%)	CaO	Al_2O_3	NiO	SiO_2	Fe_2O_3	MgO	K_2O	CuO	TiO_2	P_2O_5	SO_3
Cement (OPC 53)	60.82	6.04	0	20.43	5.23	2.99	0.96	0	0.8	0.12	2.61
GGBFS	35.24	20.02	0	34.9	1.05	6.95	0.54	0	0.72	0	0.58
Fine aggregate	0.69	6.8	0.11	84.93	4.54	0.3	1.53	0.27	0.55	0.05	0.23
Copper slag	0.8	5	0.03	35	54.35	2	0.5	0.9	0.27	0.1	1.05

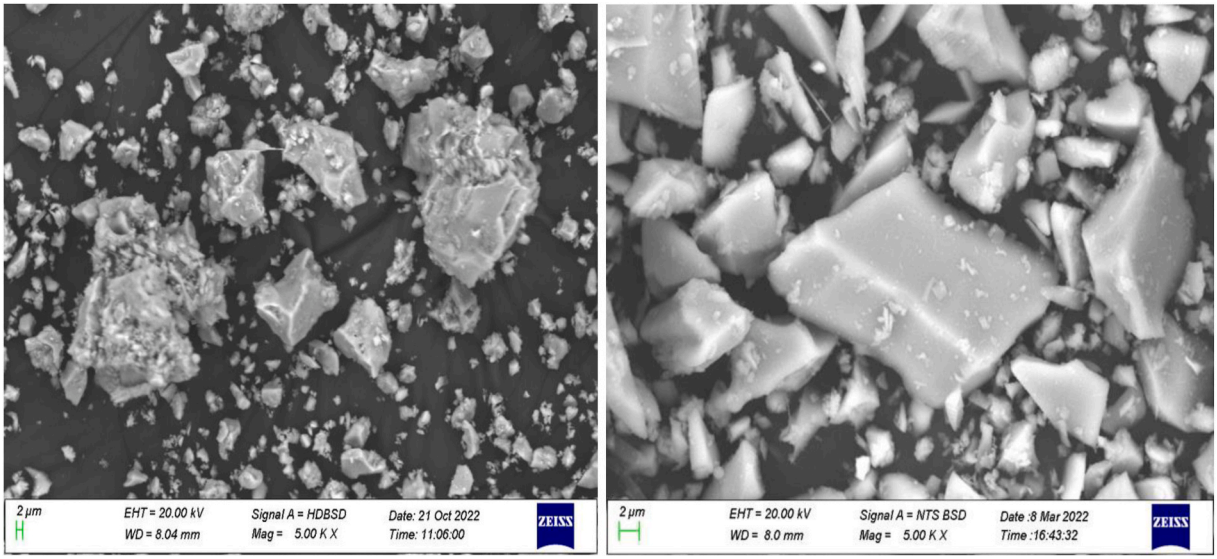

Fig. 2. Morphology of binding material.

temperature conditions: ambient temperature and elevated temperatures.

2.5. Process of thermal loading

As described in previous research work made by A. Sahu et al. [38], the water cured concrete cube specimens of 150 mm size and cylindrical specimen of size (150 X300) mm are heated in an electric muffle furnace (Fig. 4) for examining the post-heating mechanical and microstructural behaviour of concrete containing various waste materials. Several researchers have utilized thermocouples to examine the temperature gradient between the core and outer surface of concrete specimens [46–48]. However, this study focuses on post-heating conditions, where specimens are placed in a muffle furnace calibrated to reach specific target temperatures. The heating process involves a steady temperature increase at a controlled rate until the desired temperature is attained, followed by constant heating at that temperature. Subsequently, the specimens are allowed to cool naturally to room temperature. Four distinct target temperatures were considered in this study: 200 °C, 400 °C, 600 °C, and 800 °C. A uniform heating rate of 10 °C/min [28] was applied to ensure homogeneous temperature distribution within the specimens. Once the target temperature was reached, the specimens were maintained at that temperature for 2 h [7,45,46] to ensure adequate heat penetration. After exposure, the specimens were allowed to cool before testing. A complete heating and cooling cycle for the specimens at different temperature levels is illustrated in Fig. 5. This process ensured that the specimens were subjected to a controlled thermal regime within the high-temperature furnace, providing

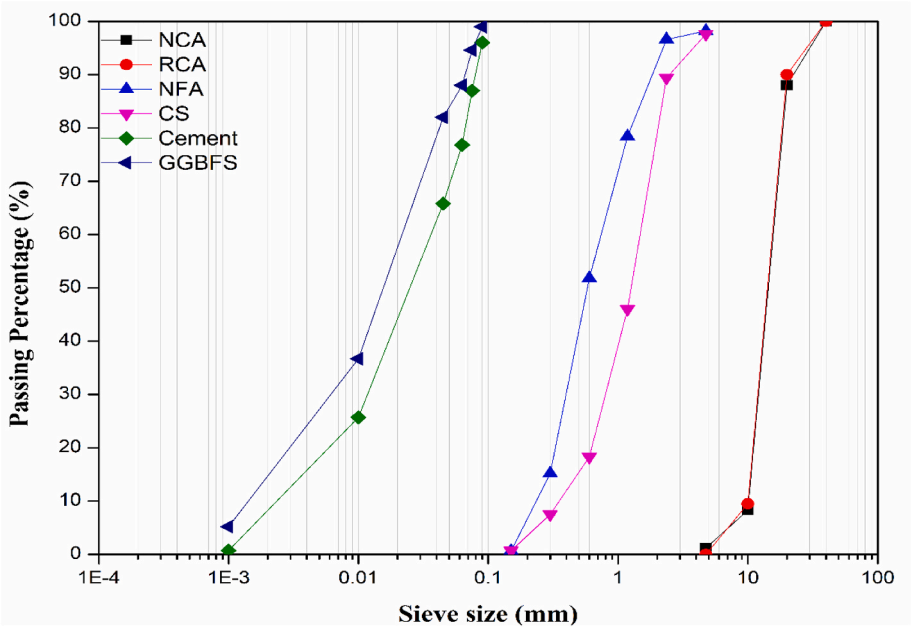

Fig. 3. Grading analysis for aggregates.

Table 3
Design mix proportions per m^3 of concrete.

Mixtures	R0C0G0	R33C0G0	R67C0G0	R100C0G0	R33C20G0	R33C40G0	R33C60G0	R33 C40G20	R33C40 G40	R33C40G60
	Mix 1	Mix 2	Mix 3	Mix 4	Mix 5	Mix 6	Mix 7	Mix 8	Mix 9	Mix 10
	Serie 1				Series 2			Series-3		
OPC (kg)	369	369	369	369	369	369	369	295	221	148
GGBFS (kg)	0	0	0	0	0	0	0	74	148	221
NFA (kg)	790	790	790	790	632	474	316	474	474	474
NCA (kg)	1135	761	375	0	761	761	761	761	761	761
CS (kg)	0	0	0	0	158	316	474	316	316	316
RCA (kg)	0	374	761	1135	375	375	375	375	375	375
Water (Kg)	166	166	166	166	166	166	166	166	166	166
SP (%)	1	1	1	1	1	1	1	1	1	1

*R0C0G0: concrete prepared with 0 % RCA 0 % CS and 0 % GGBFS.

sufficient time for heat penetration before cooling.

2.6. Mechanical properties

Mechanical properties of various concrete mixes are assessed by performing compressive and split tensile strength test at elevated temperatures followed with IS 516: 2021 [49]. For conducting compressive strength test, 150 mm size of cube specimens are subjected to 3000 KN compression testing machine with loading rate of 14 N/mm^2/min. In order to test for split-tensile strength, 150 × 300 mm cylindrical specimens are continuously loaded at a rate of 1.2 N/mm^2/min. For evaluating modulus of elasticity, the extensometer with strain gauge is attached in the longitudinal direction of cylindrical specimens of (150 x 300) mm dimension as per the provision of IS 516: 2020 [50].

3. Analysis of the results

3.1. Fresh properties of concrete

The fresh properties of different series of concrete mixes are determined from slump cone test confirming to IS 7320:1974 [51] and the slump values of different mixes are presented in Fig. 6. The first series shows the slump of RCA mix including control mix whereas the second and third series of mix showed the slump of CS blended with RAC mix and GGBFS blended with CS and RAC mix. As

Fig. 4. Muffle furnace used in the study.

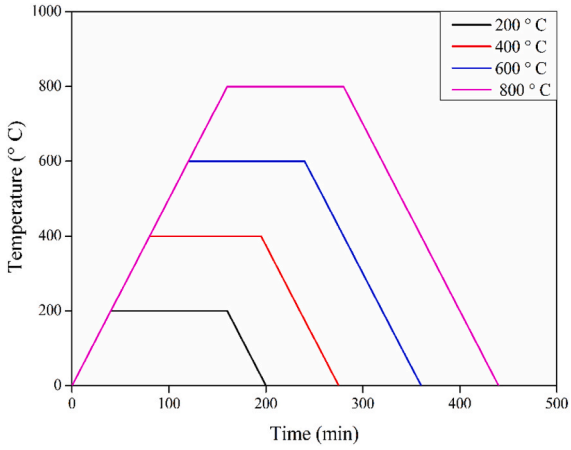

Fig. 5. Heating & cooling process at different temperature exposure.

observed from Fig. 6, the slump value of concrete in the third series of mix (when GGBFS is added to the RCA and CS mixes) showed superior results as compared to the other two series of mix. With the addition of GGBFS from 20 to 60 % the slump of concrete is increased up to 67 %, 58 % and 20 % respectively over control, RAC and CS blended RAC mix. The lubricating effect of the fine, irregular and glassy structure of GGBFS particles decreased internal friction among the components of the concrete and improved the slump behaviour by filling voids and enhancing particle dispersion [37]. The addition of GGBFS also improved the packing efficiency of the mix by reducing void content and optimizing particle arrangement, leading to a **higher slump value** [52–54].

3.2. Compressive strength of RAC at different temperature exposures

In order to determine the influence of RCA, CS and GGBFS on the strength properties of RAC subjected to thermal exposures, the compressive strength of RAC with different blends are evaluated after 28 days of water curing and at different temperature exposures with corresponding mass loss.

3.2.1. Influence of RCA

The compressive strength of RAC at various temperature exposures with corresponding mass loss when RCA is substituted in various fractions for NCA is graphically represented in Fig. 7(a).

where RCA is substituted in different fractions for NCA. Fig. 7 (a) illustrated that; the compressive strength of RAC declined when the temperature is rose from 30 to 800 °C. The strength of RAC is reduced up to 24.51 %, 27.42 %, 29 %, 33 % and 29 % at the exposure

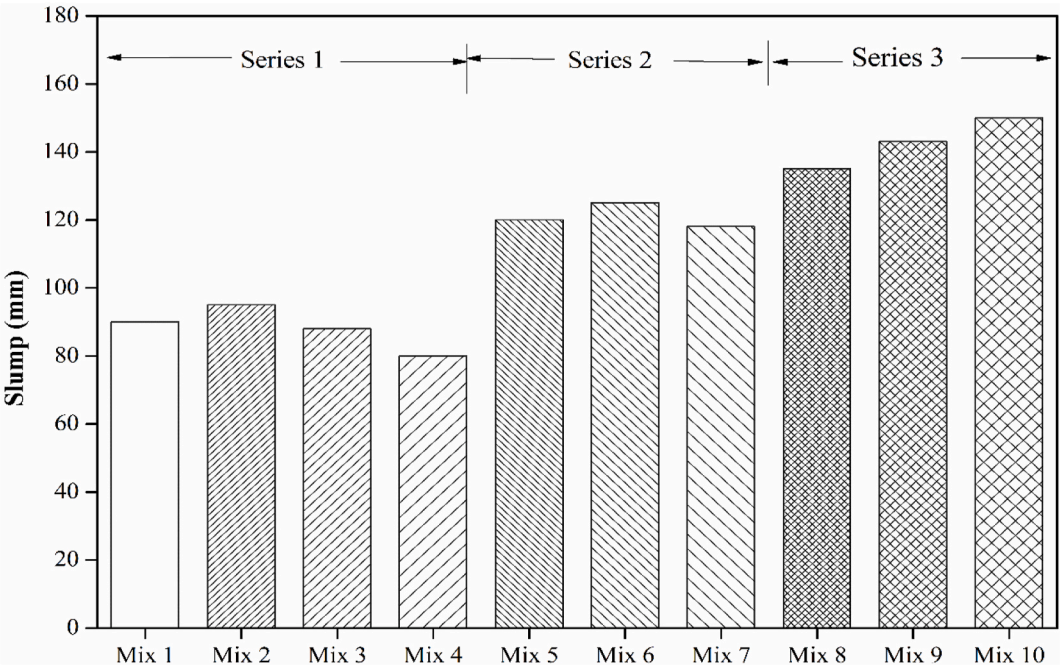

Fig. 6. Slump value of different concrete mixtures.

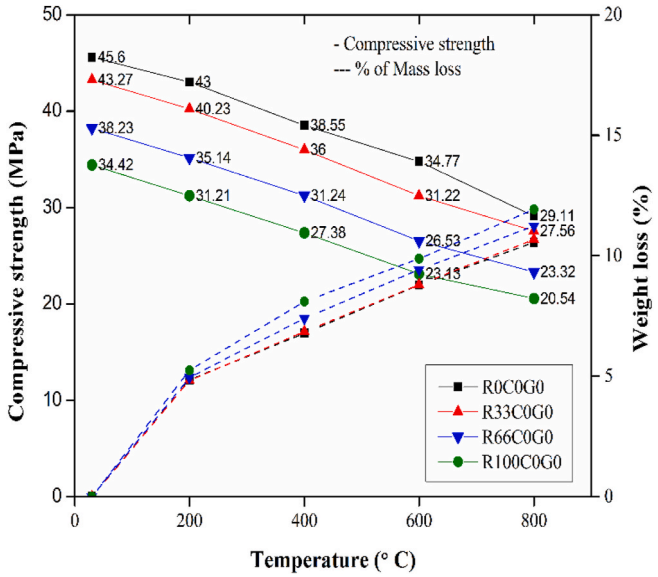

(a) Compressive strength of RAC with mass loss at varying temperature

Fig. 7 (a). Compressive strength of RAC with mass loss at varying temperature.

of 30, 200, 400, 600 and 800 °C respectively after substitution of RCA as NCA up to 100 %. Similar observations are made by Salahuddin et al. [9] at same proportion of RCA. The dehydration with breakdown of hydrated products, coarsening of pore structures and temperature differentiation in aggregates is the primary cause of strength loss in RAC with raised temperature [55]. Similarly, The mass loss rate is increased in RAC mixes after temperature exposure of 400 °C–800 °C as there was heavy water loss in RAC than normal concrete [9,37]. The larger adherent mortar surrounding the RCA surface and its higher water-absorbing capacity enhances the mass loss in RAC mixes at any given temperature as compared to the control specimen. Fig. 7 (b) depicts the effect of RCA at various

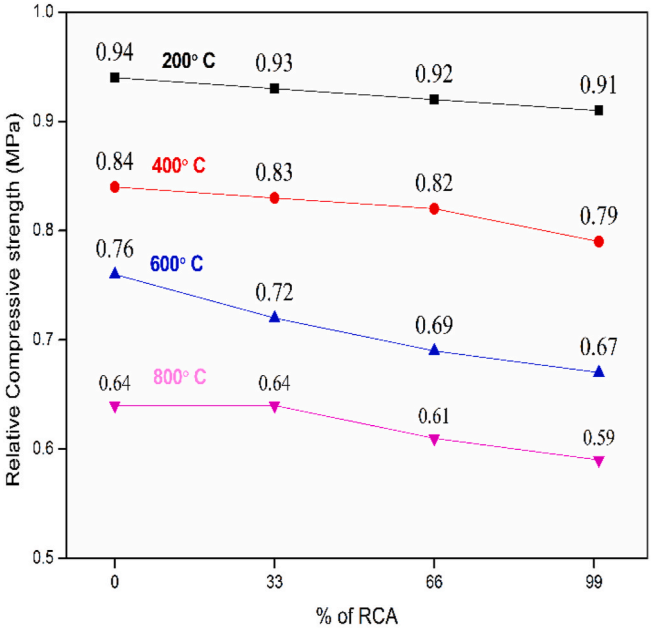

(b) Relative compressive strength at different replacement % of RCA

Fig. 7 (b). Relative compressive strength at different replacement % of RCA.

replacement levels on relative compressive strength of RAC at various temperature exposures. The relative values of compressive strength of all RCA mixes after different temperature exposures were calculated in relation to their strength at room temperature. Fig. 7 (b) clearly indicated the decreasing trend of relative compressive

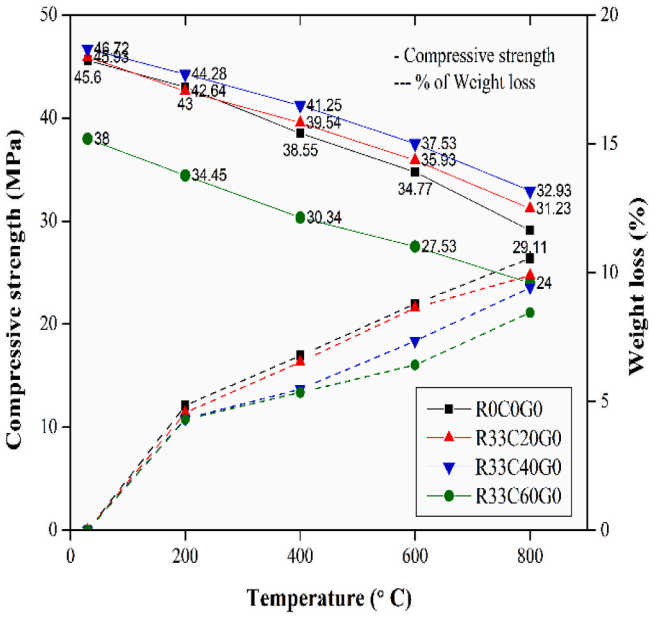

(a) Compressive strength of CS-RAC mixes at varying temperatures with mass loss

Fig. 8 (a). Compressive strength of CS-RAC mixes at varying temperatures with mass loss.

strength with the increased RCA percentage and the decreasing rate is more significant at high temperature exposures. However, the RAC mix with 33 % RCA exhibited marginal reduction rate of relative compressive strength as compared to control and other RAC mixes irrespective of all temperatures as the amount of mortar adhere to the RCA surface improved the thermal expansion characteristics between the binders and aggregate [21].

3.2.2. Influence of CS

Fig. 8 (a) shows the compressive strength of CS-RAC mixes at different temperature exposures where copper slag is replaced the fine aggregate up to 60 % and combined with 33 % RCA. The findings from Fig. 8 (a) indicated that, with the increased temperature from 30 to 800 °C the compressive strength of CS-RAC combinations dropped. However, the CS incorporation enhanced the RAC's residual compressive strength over control mixture. The maximum residual strength (up to 13 %) is attained by the RAC with 40 % CS from 30 to 800 °C. As CS particles have lower thermal expansion characteristics and a lesser propensity to absorb water than NFA, the CS based RAC mixtures exhibited greater strength than control mixture (R0C0G0) as they generate comparatively fewer voids and cracks at higher temperatures. Similarly, the CS blended RAC specimens exhibited minimum weight loss at different temperature condition in comparison to the control and RAC mix because of its lower water absorption properties than NFA which improved the thermal compatibility between the and aggregate [32]. The weight loss of RAC mixes decreased by up to 26 % with the increased CS content that emphasises the beneficial impact of CS for mass detaining RAC in high exposure scenarios. From Fig. 8 (a) it is also noticed that, with the increased temperature the CS mixes

showed reduced compressive strength with respect to its initial strength which may be due to the chemical degradation at high temperatures along with deterioration of the microstructure [15]. The effect of various replacement of CS on relative compressive strength of CS-RAC is represented in Fig. 8 (b) which shows increasing trend of strength with an increase amount of CS from 0 to 40 % irrespective of all temperature conditions. Further, when the CS content increased to 60 % the RAC's relative compressive strength decreased by 12 %.

3.2.3. Influence of GGBFS

The compressive strength of GGBFS blended CS-RAC mixes at different temperature exposures are displayed in Fig. 9 (a) with corresponding mass loss. As observed from Fig. 9 (a), all the mixes exhibited a decrease in compressive strength with the increased temperature due to the continuous dehydration and break down of hydrated products. The incorporation of GGBFS however boosted the residual compressive strength of CS-RAC mixtures over control mix. The residual strength is increased to 8 % and 19 % after the exposure of 800 °C with the inclusion of 20 % and 40 % GGBFS respectively. The pozzolanic interaction between GGBS and Calcium

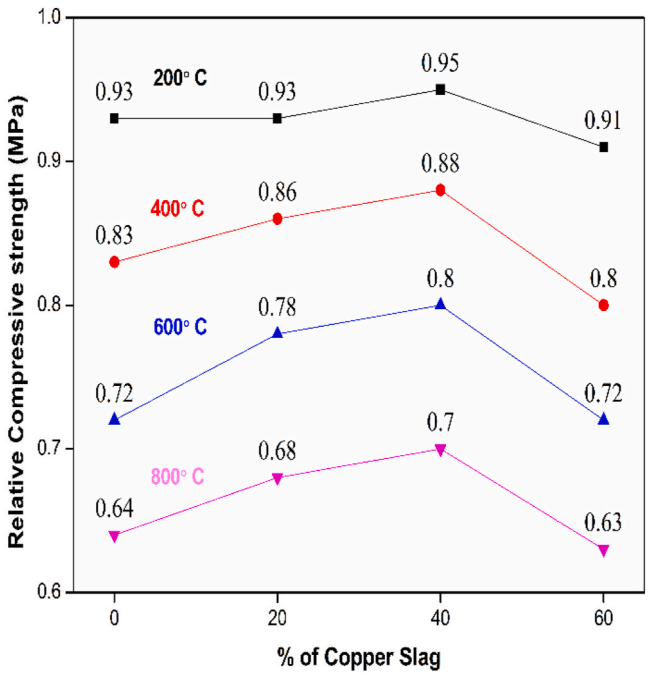

(b) Relative compressive strength at different replacement % of CS

Fig. 8 (b). Relative compressive strength at different replacement % of CS.

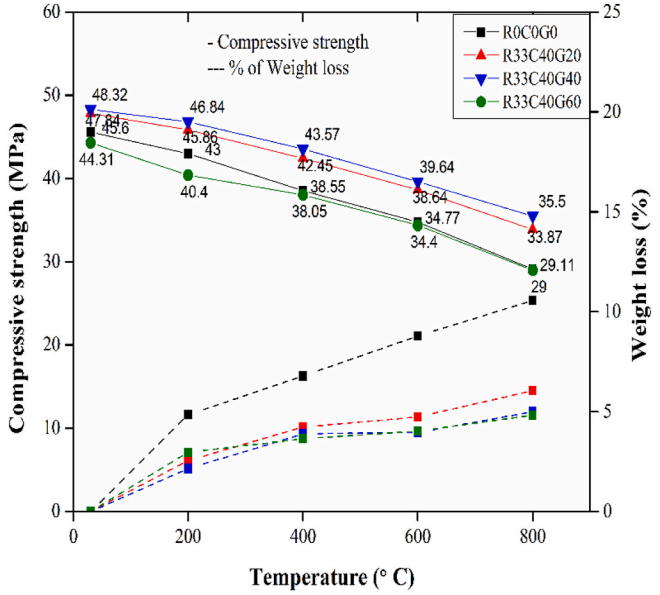

(a) Compressive strength of GGBFS blended CS-RAC mixes at varying temperatures with mass loss

Fig. 9 (a). Compressive strength of GGBFS blended CS-RAC mixes at varying temperatures with mass loss.

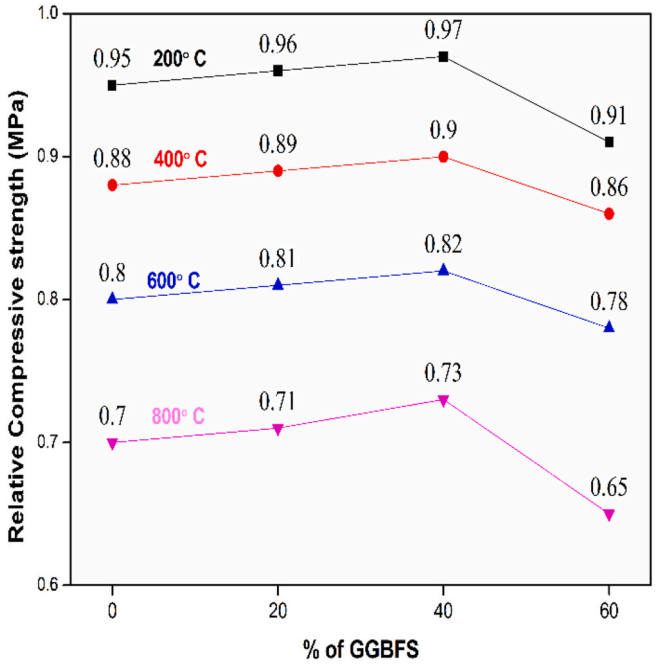

(b) Relative compressive strength at different replacement % of GGBFS

Fig. 9 (b). Relative compressive strength at different replacement % of GGBFS.

hydroxide in GGBS-RAC combinations and the additional hydration of non-hydrated cement particles boosted the strength of the mix [37,56]. Similar findings were observed by Tung et al. [37], where the inclusion of 40 % GGBFS to RAC experienced higher residual compressive strength than that of RAC without GGBFS. The GGBFS blended CS-RAC specimens experienced least mass loss as observed from Fig. 9 (a) with the addition of 20 % GGBFS and the rate of reduction is increased up to 56 % when the amount of GGBFS is increased to 60 %.

The impact of GGBFS replacements on the relative compressive strength of CS-RAC is displayed in Fig. 9(b) indicating that adding GGBFS escalated the relative strength of CS-RAC under all exposure conditions and the strength increases as the amount of GGBFS increases up to 40 %. The formation of additional hydration products by pozzolanic reactions between GGBFS particles and RCA increased this strength. The CS-RAC containing 60 % GGBFS experienced least relative compressive strength in comparison to 20 % and 40 % GGBFS due to excessive fineness of GGBFS at higher replacement level that increased the mobility of un-hydrated GGBFS particles and acted as a non-reactive ingredient in CS-RAC mixture which caused early failure during compressive strength testing [37].

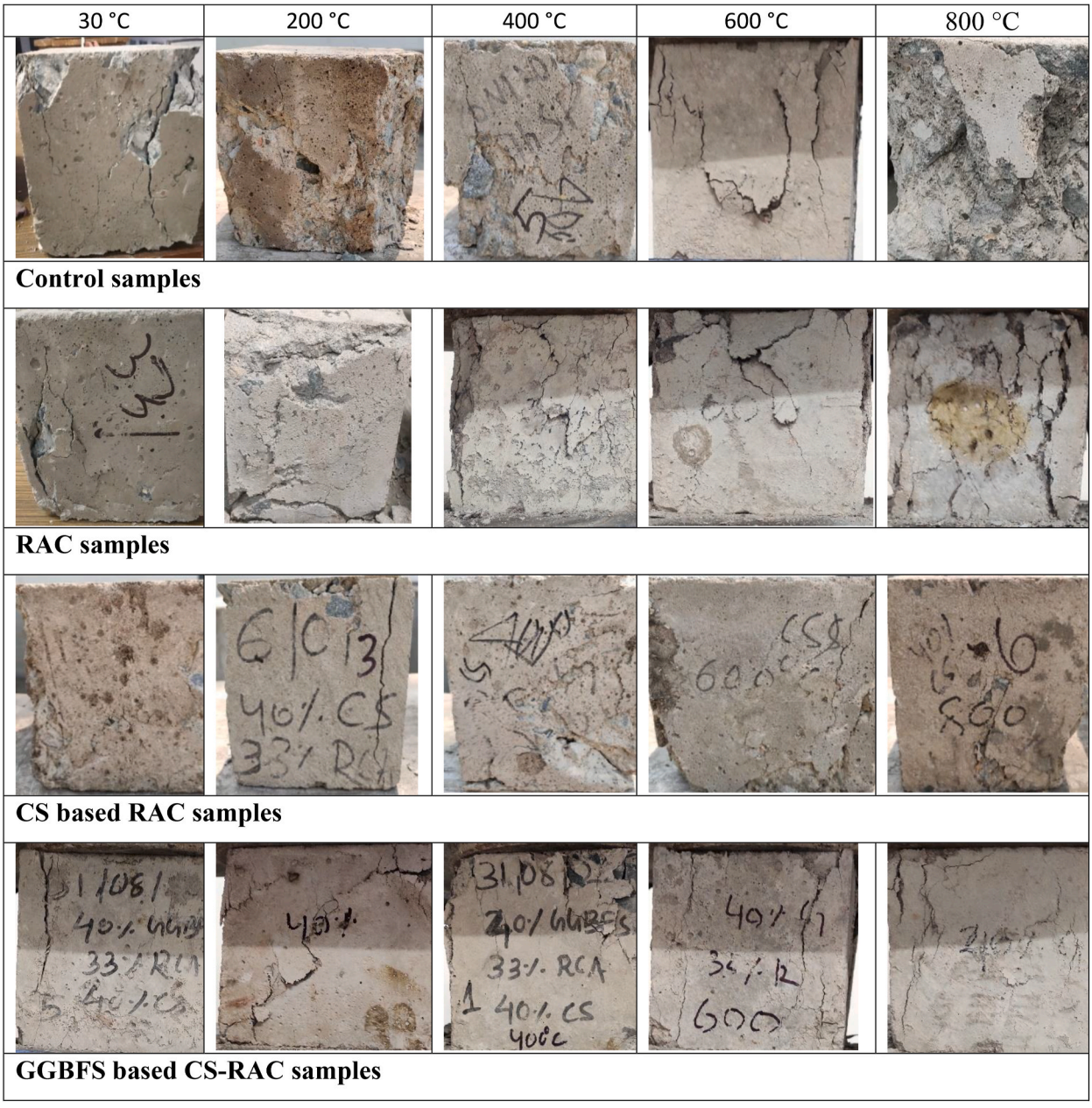

Fig. 10. Compression failure of concrete samples at ambient and elevated Temperatures.

3.3. Cracks pattern after compression failure

Fig. 10 shows the failure pattern of different concrete samples subjected to compression at room and exposure to high temperatures. A common failure mode was noticed in all concrete samples at ambient temperature. The crack patterns observed were very narrow and small. After temperature exposure of ≥400 °C, the control and RAC samples showed severe cracks rather than CS-RAC samples and GGBFS based CS-RAC samples. This was because of the high vapor pressure that caused thermal cracks to emerge during the heating process, which were irreparable after the cubes cooled. As shown in Fig. 10, the control and RAC samples developed patterned concentrated cracks and explosive spalling on their surface at temperatures of 600 and 800 °C due to the presence of intense heat pockets which caused tiny layers to chip off (iqbal et al., 2020). However, when CS and GGBFS were added to the RAC mix the internal structure was more stable against thermal effects at higher temperature due to their filling effects and cause less cracks during compression failure. Additionally, at elevated temperature the cracking pattern of the RAC containing CS and GGBFS is uniformly distributed and has closer spacing compared to the control sample (R0C0G0) and RAC sample (R33C0G0) which exhibits growing and wider cracks. This is because GGBFS prevents more $CaCO_3$ from forming in the cement paste at high temperature exposures leading to less $CaCO_3$ breakdown at higher temperatures and development of small fissures on the surface of GGBFS based CS-RAC samples [57].

3.4. Split-tensile strength

Fig. 11 shows a graphical representation of the split-tensile strength findings after 28 days for various blends at different exposed temperatures. As the temperature increased from 30 to 800 °C all the mixes exhibits reduced split tensile strength relative to its initial temperature [38]. Nevertheless, the reduction is lessened when GGBFS is included in the RAC mixture. For example, relative to the initial temperature the control mix's tensile strength decreased by roughly 5.6 % at 200 °C, 23.4 % at 400 °C, 45 % at 600 °C and 63 % at 800 °C exposure respectively.

The addition of GGBFS however decreased the tensile strength of RAC by 1.92 %, 12.62 %, 24.87 %, and 43.34 %, respectively, under the same temperature conditions. Notably, the control samples consistently exhibited the lowest splitting tensile strength across all tested increased temperature ranges. According to the researchers' findings [21,58], similar results are found at high temperature exposures. This is likely because the cement pastes in RAC and the old attached mortar have similar coefficients of thermal expansion, making tensile strength more vulnerable to heat and microcracks, which are less common in RAC than in regular concrete. Additionally, the splitting strength of CS-RAC mix increased remarkably in comparison to RAC mix after addition of GGBFS up to 60 % at all tested temperatures. The strength is increased by 26.4 %, 42.7 %, and 19.1 % respectively over RAC mix (R33C0G0) and by 12 %, 26.4 % and 5.47 % respectively over CS blended RAC mix (R33C40G0) at the exposure of 800 °C when 20 %, 40 %, and 60 % GGBFS were added. GGBFS enhanced the binding strength between the RCA and fresh cement paste, which boosted the tensile strength of CS-RAC mixtures [35].

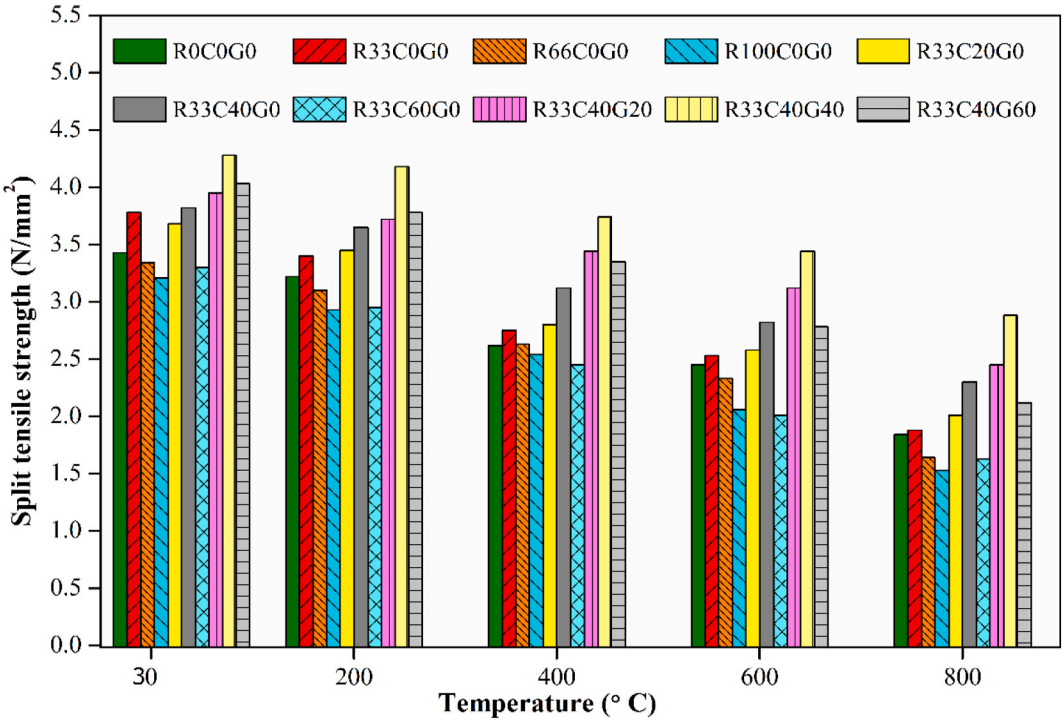

Fig. 11. Split tensile strength of several series of mixtures at varying temperatures.

3.5. Modulus of elasticity

The variation of modulus of elasticity of different series of concrete mixes at different temperature exposures are presented in Fig. 12. It has been noticed that; all the series of concrete mixes exhibit decreased modulus of elasticity with the elevated temperature from 30 to 800 °C. The modulus of elasticity of control mix is continuously increased in comparison to RAC mixes at ambient and after high temperature exposure as the elasticity modulus of natural aggregates is higher than that of RCA because of the latter's intrinsic fissures and significant porosity [37]. After being heated to 800 °C, the modulus of elasticity of the RAC mix with 33 % RCA drops by up to 16 % compared to the control mix. Similarly, the RAC mixes containing 66 % and 100 % RCA exhibited 36 % and 48 % decreased modulus of elasticity over control mix. The continuous decrease in modulus of elasticity at higher temperature in comparison to control concrete is mainly due to the internal microcracks of cement paste bonded to the surface of RCA caused by thermal stresses, where the higher cracking state facilitates the transfer of stresses, delaying material rupture [7]. Moreover, at higher temperature the RAC mixes exhibited high water loss due to evaporation resulting the formation of large number of voids and cracks compared to control concrete and rapid breakdown of hydrated calcium silicate gel (CSH) decreased the bonding characteristics of RAC and reduced their elasticity modulus. However, the addition of CS and GGBFS increased the modulus of elasticity of RAC mix (R33C0G0) under all exposure conditions. The RAC's elastic modulus enhances by 23 % over control mix when CS is added up to 40 %, while the inclusion of GGBFS up to 60 % increased the elastic modulus by 45 % when the exposed temperature rose from 30 to 800 °C. R33C40G40 mix experienced higher modulus of elasticity at all tested temperature exposures. The higher thermal properties of CS and GGBFS than that of NFA and cement reduces the development of cracks in RAC at higher temperatures and improved its modulus of elasticity. Additionally, the pozzolanic effect of GGBFS causes less disintegration at the interfacial transition zone, producing more C-S-H hydrates. This increased the bonding characteristics of GGBFS based RAC mixes at higher temperature, increasing their stiffness and modulus of elasticity [37].

To establish the relation among residual compressive strength, residual splitting tensile strength and modulus of elasticity, a linear regression is carried out by considering test results at different temperature exposures and presented in Fig. 13. A strong and direct correlation with $R^2 = 0.99$ is observed between residual tensile strength and compressive strength values, suggesting that the residual split tensile strength of all RAC mixtures decreases as the residual compressive strength decreases. Similarly, a direct linear correlation is found between test results of residual compressive strength and residual modulus of elasticity with $R^2 = 0.98$.

3.6. XRD analysis

X-Ray Diffractogram analysis of different concrete mixes were carried out both at ambient and elevated temperature condition to examine the various hydrated phases like portlandite [Ca $(OH)_2$], quartz (SiO_2), ettringite ($3CaO.Al_2O_3.3CaSO_4$, $3H_2O$), calcium silicate hydrate (CSH) and calcite ($CaCO_3$) present within the core matrix. The XRD test was performed at NIT in Durgapur, India, for

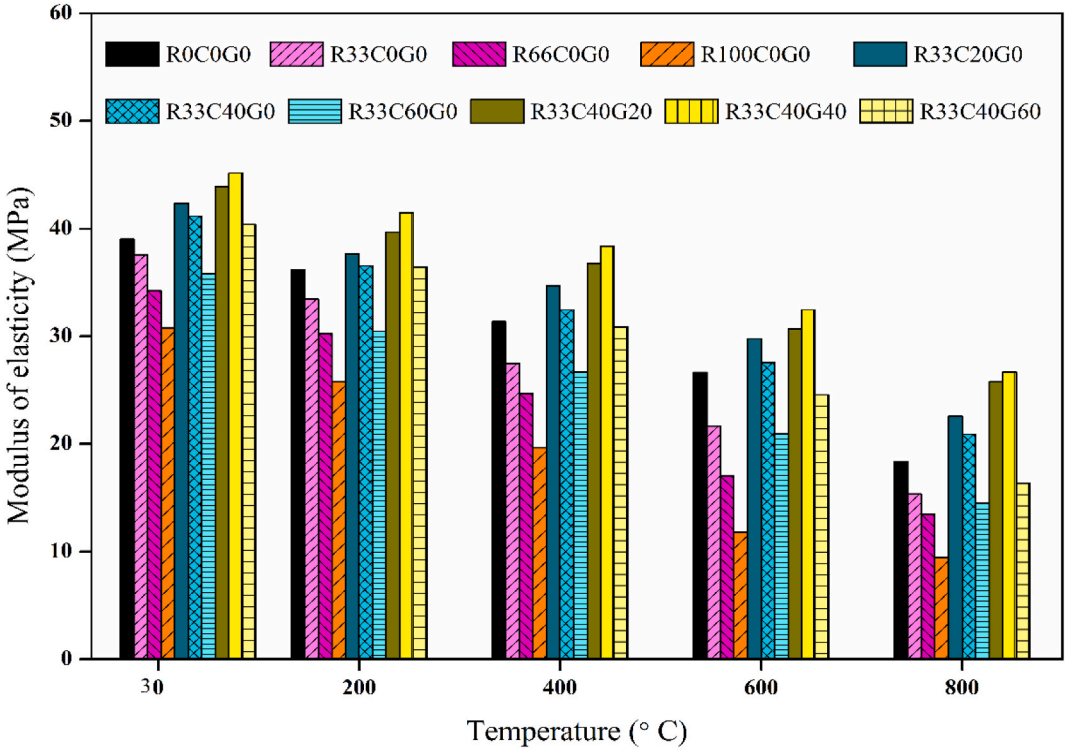

Fig. 12. Modulus of elasticity of several series of mixtures at varying temperatures.

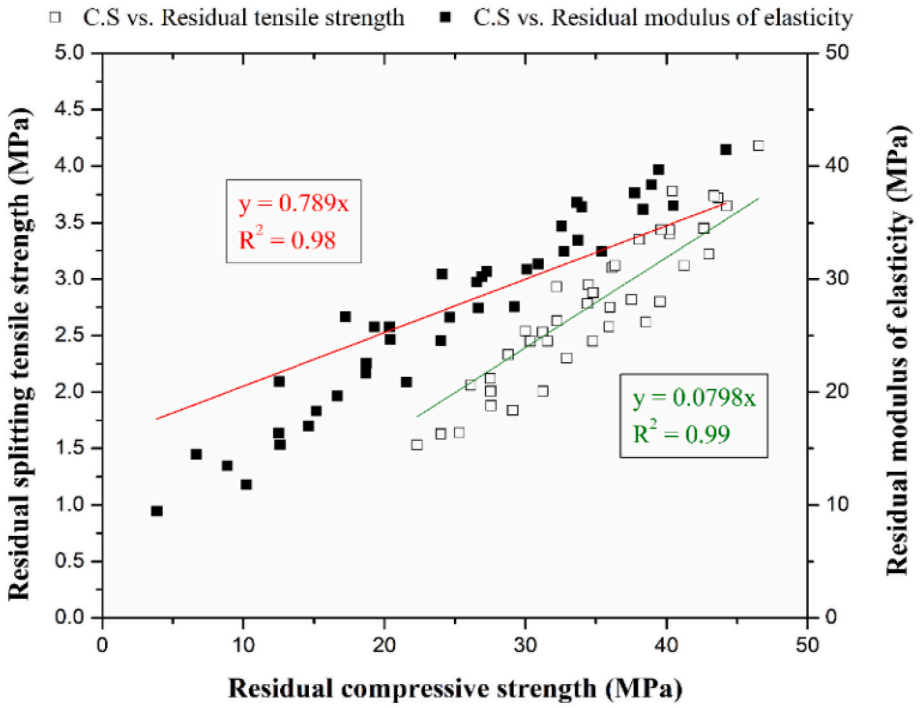

Fig. 13. Linear regression among residual compressive strength, splitting tensile strength and modulus of Elasticity.

this investigation. The fractured pieces obtained from crushed concrete followed by compressive strength test was grinded in to powdered form, sieved through 90-μm sieve, and placed on diffractometer for XRD test.

In the present study XRD test has been performed for control mix (R0C0G0), recycled aggregate mix (R33C0G0), copper slag blended recycled aggregate concrete with 40 % CS content (R33C40G0) and GGBFS blended with copper slag based recycled aggregate concrete with 40 % GGBFS content (R33C40G40) at the exposed temperature of 30 °C (Room temperature) and 800 °C which is represented in Figs. 14 and 15 respectively. The analysis has been carried out for 2ɵ angles ranging from 10° to 70°. As observed from Fig. 14, at ambient temperature, the XRD pattern of concrete mixtures confirmed the crystalline phases at various replacement level. The major peak showed the significant crystalline phases of Quartz in all the concrete mixtures which is observed at 2ɵ angle of 26.65°. The control mix (R0C0G0) observed a clear and distinct crystalline phases of ettringite and calcite with the traces of CSH that enhances the strength of concrete. However, comparatively weaker phases of calcium sulpho aluminate and CSH has been observed in RAC mix (R33C0G0) which causes the strength reduction. The existence of calcium hydroxide phase in RAC also reduced the strength as it develops cracks and voids inside the matrix. Nevertheless, CS and GGBFS boosted the formation of CSH and created a compact structure when they were added to the RAC mix. Fig. 14 showed the major crystalline phases of Calcite, Quartz and Gismodine in R33C40G0 mix that made the microstructure more compact and escalates the strength of the mix. Gismodine ($CaAl_2Si_2O_84H_2O$) is a monoclinic crystalline structure forms colourless, bipyramidal crystals that found only in the RAC mixtures containing copper slag. In addition, the existence of Belite (C_2S) formed CSH gel in the mixture. The RAC mixes containing 40 % CS and 40 % GGBFS (R33C40G40) exhibited the significant peaks of Quartz and Gismodine which developed a compact microstructure in comparison to the other mixes. In addition, Gehlenite ($Ca_2Al_2SiO_7$) and Akermanite ($Ca_2MgSi_2O_7$) phases were found only in R33C40G0 mix containing GGBFS which are used to fill the pores and voids developed in RAC mix (R33C0G0) and increased the strength. However, the existence of portlandite and calcite phase developed the pozzolanic activity of GGBFS in R33C40G40 mix which again enhanced the strength of RAC.

Fig. 15 depicts the XRD analysis of different concrete mixtures at the exposure of 800 °C. The crystalline phase of ettringite was vanished in all the mixtures as it became unstable at higher temperature and completely decomposed. The crystalline phase of CSH gel disappeared as it completely decomposed at 600 °C. However, all the mixtures exhibit increased crystalline phase of Quartz as observed in Fig. 15 which is attributed to the decomposition of other cementitious phases (Portlandite, Ettringite and CSH), leading to a higher relative percentage of Quartz in remaining solid mass. Further, the diffractogram of control and RAC mix noticed Calcite phase that developed number of pores and voids inside the matrix at higher temperature and degrades the concrete strength. The mix R33C40G0 exhibit the crystalline phases of Gismodine, Quartz and Belite that made the mix more compact. However, with respect to initial temperature the strength degradation is more in R33C40G0 mix when exposed to high temperature due to continuous dehydration of Calcium Hydroxide (Portlandite) and CSH phase. Whereas, when GGBFS is included in CS-RAC mix the Gehlenite phase appears which could repair the internal damage and fill the wider pores in RAC that are created by high temperatures and increased the residual strength [46,59]. Furthermore, the existence of Akermanite crystalline phase in R33C40G40 reduced the thermal conductivity

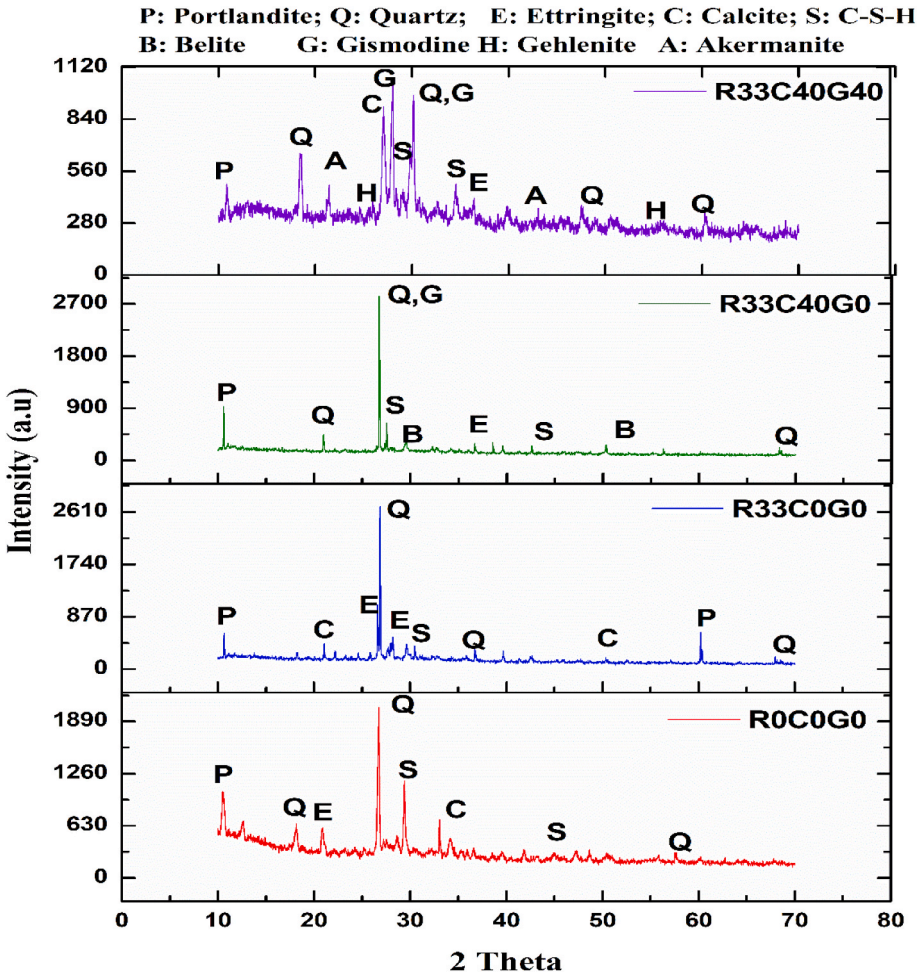

Fig. 14. XRD analysis of concrete mixes at 30 °C.

of RAC and enhanced its residual properties with mild thermal damage [46].

3.7. SEM analysis

To examine the surface features of crushed concrete sample, such as the arrangement of different hydrated and un-hydrated products, a SEM investigation was conducted on the cement matrix. In the present study SEM has been performed for control mix (R0C0G0), recycled aggregate mix (R33C0G0), copper slag blended recycled aggregate concrete at 40 % CS content (R33C40G0) and GGBFS blended with copper slag based recycled aggregate concrete at 40 % GGBFS content (R33C40G40) at the exposed temperature of 30 and 800 °C and studied their microstructure performances. Fig. 16(a–d) shows the SEM image of various concrete mixes at ambient temperature condition. The morphology of control mixes as shown in Fig. 16 (a) exhibits a compact and dense structure. Throughout the sample, the calcium silicate hydrate (CSH) crystals are precisely dispersed and positioned. The image also shows distinct microcracks associated with the ettringite development. Fig. 16 (b) displays the micrograph examination of the RAC matrix created using 33 % RCA. Compared to the control mix, microstructure of the RAC matrix was less compact and crystalline. Amorphous CSH crystals are visible all throughout the image, indicating their creation. The existence of pores and voids in the RAC matrix lower its thermal conductivity relative to the control concrete because of the increased porosity of RCA [20]. The micrograph of the CS mix (Fig. 16 (c)) revealed a thick and crystalline microstructure in contrast to the control and RAC mix. This was caused by the production of more compact CSH gel, which increased the compressive strength of RAC. The hydrated products formed a solid bond with the aggregates and were evenly distributed throughout the matrix. The porous nature of RCA attributed to the development of micro-cracks and voids in the matrix as seen in the micrograph. Similarly, the morphology of GGBFS mix (R33C40G40) is shown in Fig. 16 (d) indicating a relatively thick and compact microstructure than other mentioned microstructures. The pores and voids present in the microstructure are filled with small, un-hydrated GGBFS particles which made the structure more compact with the formation of dense CSH gel in the matrix that enhances the concrete strength.

The microstructure of concrete mixes exposed to 800 °C, depicted in Fig. 17, showed bigger cracks and voids in all mixes in

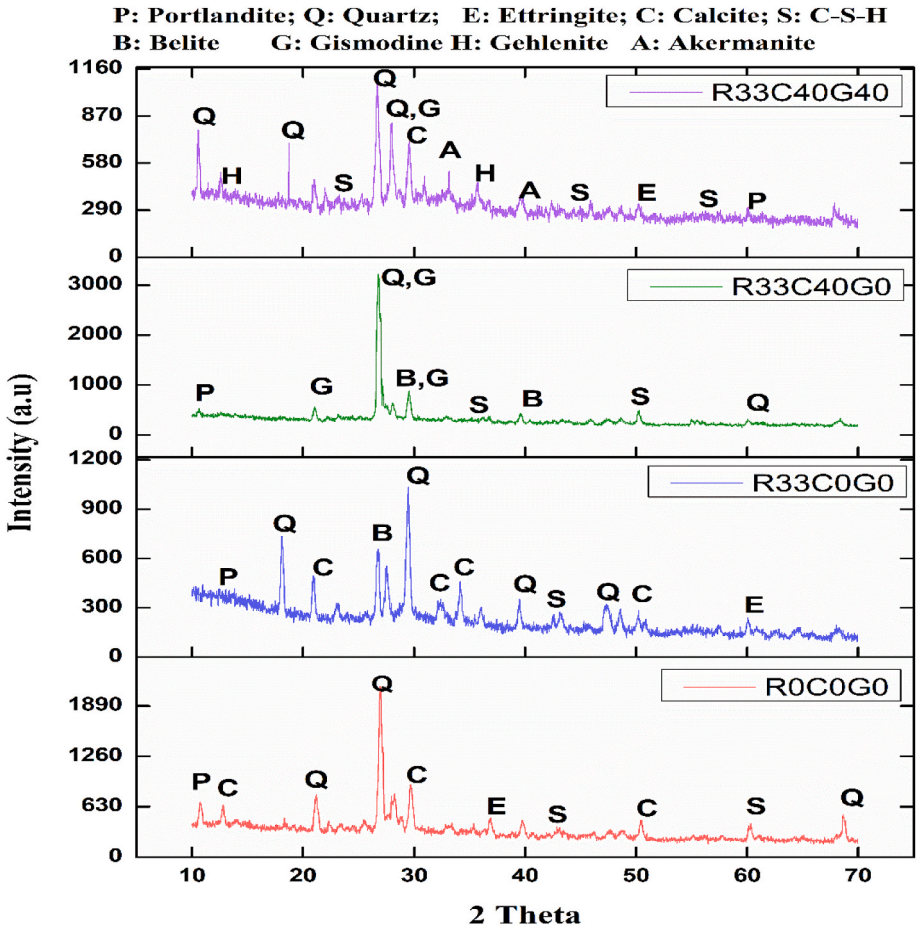

Fig. 15. XRD analysis of concrete mixes at 800 °C.

comparison to room temperature as evaporation causes at this temperature leading to reduction of strength properties [60]. Moreover, the microstructure of the control and RAC mix is significantly damaged at 800 °C due to the more noticeable breakdown of hydration products. This is consistent with Shumuye et al.'s findings [57]. As seen in Fig. 17 (a) and 17 (b), free water evaporates to form voids and pores and the enhanced porosity may have contributed to the mass loss of the RAC mix. This suggests that RCA replacement alone does not significantly reduce the residual mechanical strength at higher temperature. The micrograph of R33C40G0 matrix as seen in Fig. 17 (c) after being exposed to 800 °C showed a dense microstructure where the hydrated CSH gel is dispersed throughout the picture. Comparatively less voids and micro-cracks are formed in CS mix than RAC

mix as CS particles absorb less water than NFA and RCA.This property enabled the mortar to adhere to aggregate surfaces with greater efficiency and enhanced the ITZ characteristics, thus improved the residual mechanical strength in R33C40G0 compared to R0C0G0 and R33C0G0 specimens. However, R33C40G40 matrix as seen in Fig. 17 (d) exhibited more stabilized and denser microstructure compared to all other mixes at higher temperatures. The hydrates of CH and CSH are became more fractured and scattered in comparison to control and RAC mix with the ettringite that forms a bridge between the hydrates of CH and CSH crystals, resulting in less voids and fractures at higher temperatures. Further, when GGBFS and cement are mixed in the R33C40G40 matrix, the internal structure is strengthened against thermal effects, which leads to form lesser number of pores and fractures after high temperature exposures. This has improved the specimen's residual mechanical strength performance with respect to R0C0G0, R33C0G0 and R33C40G0 specimens at higher temperature. Thus, the study inferred that the post fire behaviour of R33C40G40 is superior in comparison to the R0C0G0 and R33C0G0 specimens in two ways. Firstly, the strength properties and ITZ performance is enhanced due to development of more amount of CSH hydrates and ettringite. Moreover, the formation of calcium hydrate (CH) and calcium hydroxide in GGBFS blended CS-RAC mix is comparatively less that are decomposed easily when exposed to high temperatures. Secondly, less CSH breakdown with fractures at ITZ is the consequence of lower heat transfer rates in GGBS blended CS-RAC matrix [37].

4. Conclusion

This research work examined the various properties of GGBFS and CS blended recycled aggregate concrete under different temperature exposures. The study's primary findings are as follows:

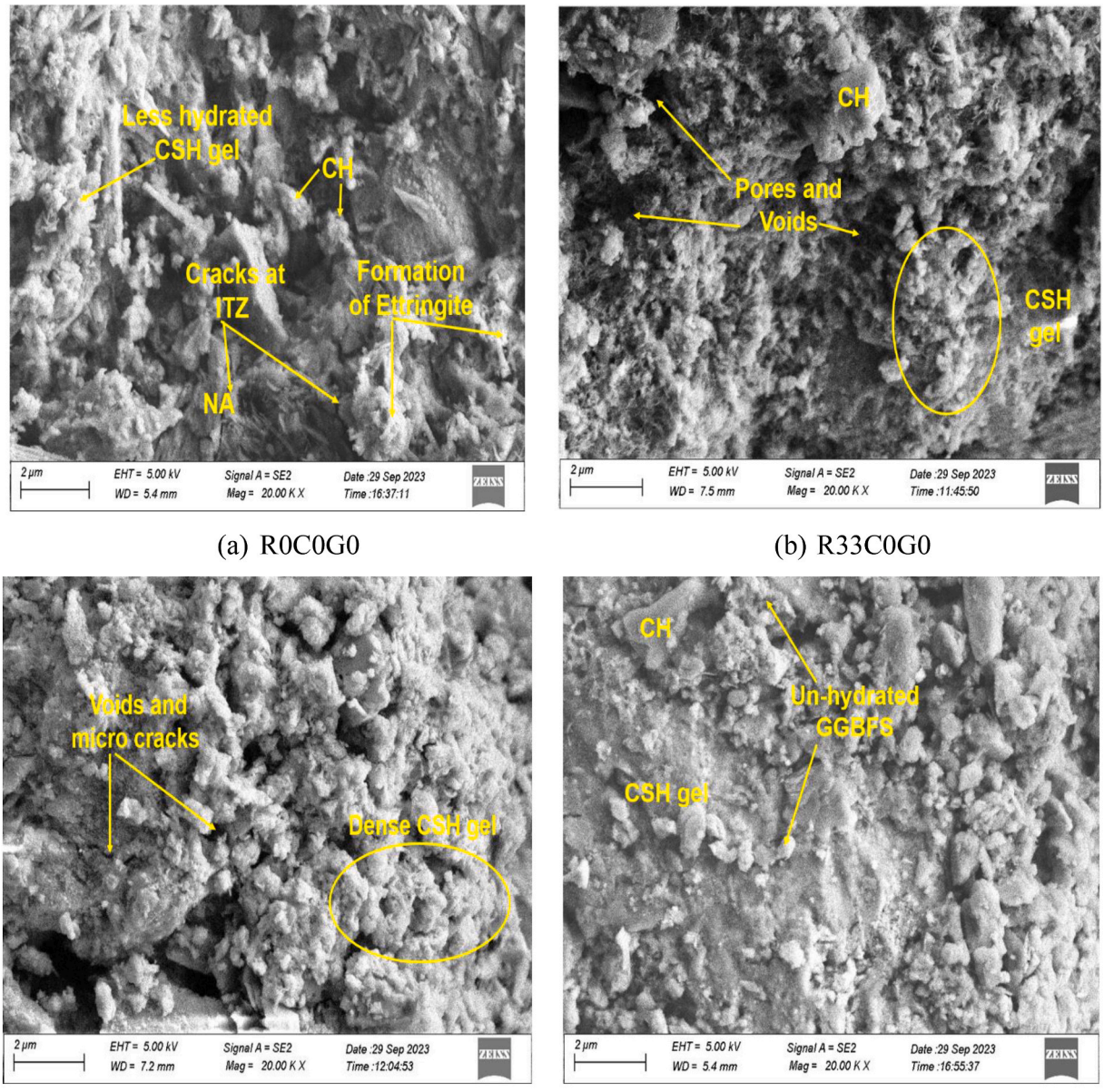

Fig. 16. SEM morphology of concrete mixes exposed at 30 °C.

1. The inclusion of CS and GGBFS enhanced the strength characteristics of RAC at room temperature. This is because of the filling action of GGBFS, making RAC denser and more compact than control mix, while CS's limited ability to absorb water makes the RCA more cohesive.

Every mix in the series showed a decrease in strength at high temperatures, and this loss increased as the temperature rose because of considerable water loss that caused pores and voids to form in the concrete matrix. However, CS and GGBFS elevated the RAC's residual performance and compared to the control concrete.

2. Incorporation of CS up to 40 % and GGBFS up to 40 % escalated the residual mechanical performance of RAC. The maximum compressive strength achieved is about 13 % and 19 % respectively while the enhanced RAC's elastic modulus is about 23 % and 47 % irrespective of all tested temperature condition. It is due to the pozzolanic properties of GGBFS along with the greater thermal properties of CS and GGBFS.

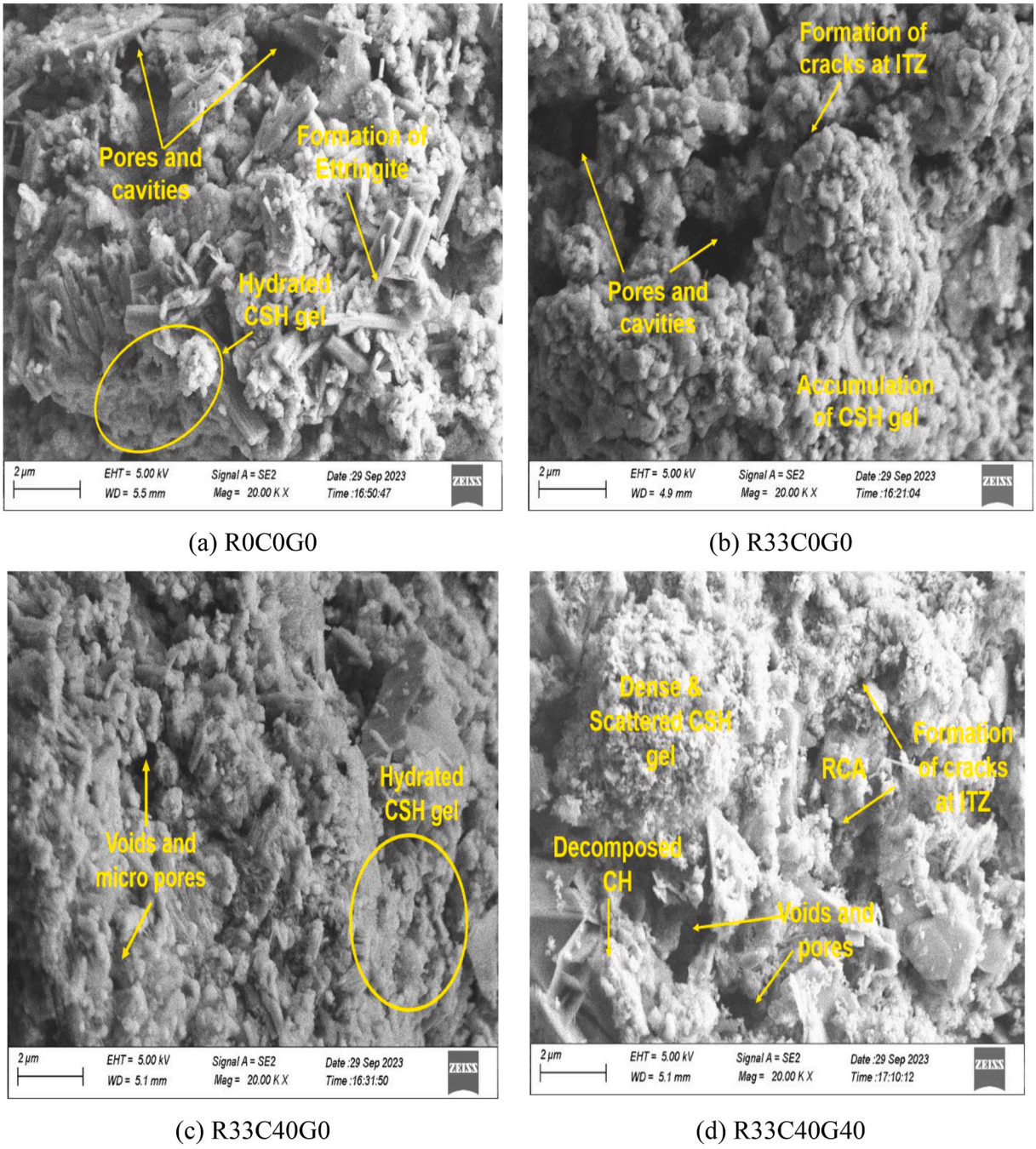

Fig. 17. SEM morphology of concrete mixes exposed at 800 °C temperature.

3. A strong relationship is established between the residual modulus of elasticity, split tensile strength, and compressive strength by linear regression analysis with $R^2 \geq 0.90$. The analysis established a direct and linear correlation between the different strength parameters.
4. The R33C40G40 concrete mix, which contained 33 % RCA, 40 % CS, and 40 % GGBFS, achieved superior residual mechanical qualities in comparison to the other mixes. It is due to (1) the improved packing efficiency (2) the pozzolanic effect of GGBFS which cause less disintegration at the interfacial transition zone and increased the bonding characteristics and stiffness of the mix.
5. The XRD analysis of different concrete mixes showed that, the existence of Akermanite and Gehlenite crystalline phase in R33C40G40 reduced the thermal conductivity of RAC and enhanced its residual properties with mild thermal damage. In addition,

the presence of Quartz and Gismodine in large amount in R33C40G40 mix developed a compact structure which escalate the strength of mixture both at room and elevated temperature.

6. The morphology of different concrete matrix showed that, the GGBFS based CS-RAC mix (R33C40G40) established a denser microstructure with fewer voids and microcracks at higher temperatures compared to other mixes. The R33C40G40 mix exhibited stable CSH gel formation which led to less C-S-H breakdown and better cement paste-aggregate bonding at high temperatures and improved the residual mechanical strength qualities of mix.

Based on the findings of the above study regarding strength and microstructural analysis, the concrete using 33 % RCA with CS and GGBFS up to 40 % shows superior performance. This research illustrates the potential of escalating the residual properties of RAC by incorporating CS and GGBFS and establishes correlations among the residual strength qualities of RAC-CS-GGBFS blends. Overall, this study makes a significant contribution to the development of sustainable concrete in civil engineering, while also improving the fire safety design of RAC.

CRediT authorship contribution statement

Anasuya Sahu: Writing – original draft, Methodology, Investigation, Conceptualization. **Sanjay Kumar:** Writing – review & editing, Supervision. **Adarsh Srivastav:** Writing – review & editing, Supervision, Methodology, Conceptualization. **Harsh Anurag:** Visualization, Investigation, Conceptualization.

Declaration of competing interest

The authors declare that they have no known competing financial interests or personal relationships that could have appeared to influence the work reported in this paper.

Acknowledgement

The authors would like to thank the faculty and staff of the Department of Civil Engineering for their advice and assistance. The National Institute of Technology (NIT), Durgapur, West Bengal, India, is also acknowledged by the authors for performing the XRD and SEM studies.

Data availability

Data will be made available on request.

References

[1] N.D. Tošić, Sustainability of the Concrete Industry – Current Trends and Future Outlook, vol. 71, 2017, https://doi.org/10.5937/tehnika1701038T.
[2] J. Sim, C. Park, Compressive strength and resistance to chloride ion penetration and carbonation of recycled aggregate concrete with varying amount of fly ash and fine recycled aggregate, Waste Manag. 31 (2011) 2352–2360, https://doi.org/10.1016/j.wasman.2011.06.014.
[3] A. Sahu, S. Kumar, A.K.L. Srivastava, B. Pratap, Performance of recycled aggregate concrete using copper slag as fine aggregate, J. Build. Eng. 82 (2024) 108364, https://doi.org/10.1016/j.jobe.2023.108364.
[4] R.K. Majhi, A.N. Nayak, B.B. Mukharjee, Development of sustainable concrete using recycled coarse aggregate and ground granulated blast furnace slag, Constr. Build. Mater. 159 (2018) 417–430, https://doi.org/10.1016/j.conbuildmat.2017.10.118.
[5] R.K. Majhi, A.N. Nayak, Production of sustainable concrete utilising high-volume blast furnace slag and recycled aggregate with lime activator, J. Clean. Prod. 255 (2020) 120188, https://doi.org/10.1016/j.jclepro.2020.120188.
[6] P. Abhishek, P. Ramachandra, P.S. Niranjan, Use of recycled concrete aggregate and granulated blast furnace slag in self-compacting concrete, Mater. Today Proc. 42 (2020) 479–486, https://doi.org/10.1016/j.matpr.2020.10.239.
[7] J. Beatriz da Silva, M. Pepe, R.D. Toledo Filho, High temperatures effect on mechanical and physical performance of normal and high strength recycled aggregate concrete, Fire Saf. J. 117 (2020), https://doi.org/10.1016/j.firesaf.2020.103222.
[8] M. Meleševv, M. Radeka, V. Radonjanin, I. Lukic, Evaluation of Sulfate Resistance of Concrete with Recycled and Natural Aggregates, vol. 152, 2017, pp. 614–631, https://doi.org/10.1016/j.conbuildmat.2017.06.161.
[9] H. Salahuddin, A. Nawaz, A. Maqsoom, T. Mehmood, B. ul A. Zeeshan, Effects of elevated temperature on performance of recycled coarse aggregate concrete, Constr. Build. Mater. 202 (2019) 415–425, https://doi.org/10.1016/j.conbuildmat.2019.01.011.
[10] M.A. Salau, O.J. Oseafiana, T.O. Oyegoke, Effects of elevated temperature on concrete with recycled coarse aggregates, IOP Conf. Ser. Mater. Sci. Eng. 96 (2015), https://doi.org/10.1088/1757-899X/96/1/012078.
[11] W. Sae-Long, T. Chompoorat, S. Limkatanyu, N. Damrongwiriyanupap, P. Sukontasukkul, T. Chub-Uppakarn, T. Thepumong, Experimental and simulation analysis of RCA and para-wood ash as partial substitutes for NCA and cement in recycled aggregate concrete, Case Stud. Constr. Mater. 21 (2024) e03716, https://doi.org/10.1016/j.cscm.2024.e03716.
[12] L.A. Qureshi, B. Ali, A. Ali, Combined effects of supplementary cementitious materials (silica fume, GGBS, fly ash and rice husk ash) and steel fiber on the hardened properties of recycled aggregate concrete, Constr. Build. Mater. 263 (2020) 120636, https://doi.org/10.1016/j.conbuildmat.2020.120636.
[13] M.J. Islam, K. Islam, M. Shahjalal, E. Khatun, S. Islam, A.B. Razzaque, Influence of different types of fibers on the mechanical properties of recycled waste aggregate concrete, Constr. Build. Mater. 337 (2022) 127577, https://doi.org/10.1016/j.conbuildmat.2022.127577.
[14] M.J. Ashraf, M. Idrees, A. Akbar, Performance of silica fume slurry treated recycled aggregate concrete reinforced with carbon fibers, J. Build. Eng. 66 (2023) 105892, https://doi.org/10.1016/j.jobe.2023.105892.
[15] E. Pawluczuk, K. Kalinowska-Wichrowska, J.R. Jiménez, J.M. Fernández-Rodríguez, D. Suescum-Morales, Geopolymer concrete with treated recycled aggregates: macro and microstructural behavior, J. Build. Eng. 44 (2021), https://doi.org/10.1016/j.jobe.2021.103317.
[16] L. Zhu, Q. Ning, W. Han, L. Bai, Compressive strength and microstructural analysis of recycled coarse aggregate concrete treated with silica fume, Constr. Build. Mater. 334 (2022) 127453, https://doi.org/10.1016/j.conbuildmat.2022.127453.

[17] J. Zhang, H. Liu, G. Liu, X. Wang, J. Geng, Q. Wang, A. Hussain, Influence on mechanical properties and microstructure analysis of hybrid fiber recycled aggregate concrete after exposure to elevated temperature, J. Adhes. Sci. Technol. 37 (2023) 2328–2347, https://doi.org/10.1080/01694243.2022.2127251.
[18] S.A. Waseem, An investigation of mechanical and durability properties of carbonated recycled aggregate concrete, J. Inst. Eng. Ser. A. 103 (2022) 349–358, https://doi.org/10.1007/s40030-021-00608-y.
[19] I. Patra, G.R.L. Al-Awsi, Y.M. Hasan, S.S.K. Almotlaq, Mechanical properties of concrete containing recycled aggregate from construction waste, Sustain. Energy Technol. Assessments 53 (2022) 102722, https://doi.org/10.1016/j.seta.2022.102722.
[20] C. Laneyrie, A.L. Beaucour, M.F. Green, R.L. Hebert, B. Ledesert, A. Noumowe, Influence of recycled coarse aggregates on normal and high performance concrete subjected to elevated temperatures, Constr. Build. Mater. 111 (2016) 368–378, https://doi.org/10.1016/j.conbuildmat.2016.02.056.
[21] S.R. Sarhat, E.G. Sherwood, Residual mechanical response of recycled aggregate concrete after exposure to elevated temperatures, J. Mater. Civ. Eng. 25 (2013) 1721–1730, https://doi.org/10.1061/(asce)mt.1943-5533.0000719.
[22] C.Q. Lye, S.K. Koh, R. Mangabhai, R.K. Dhir, Use of copper slag and washed copper slag as sand in concrete: a state-of-the-art review, Mag. Concr. Res. 67 (2015) 665–679, https://doi.org/10.1680/macr.14.00214.
[23] C.K. Madheswaran, P.S. Ambily, J.K. Dattatreya, N.P. Rajamane, Studies on use of copper slag as replacement material for river sand in building constructions, J. Inst. Eng. Ser. A. 95 (2014) 169–177, https://doi.org/10.1007/s40030-014-0084-9.
[24] A. Maharishi, S.P. Singh, L.K. Gupta, Shehnazdeep, Strength and durability studies on slag cement concrete made with copper slag as fine aggregates, Mater. Today Proc. 38 (2020) 2639–2648, https://doi.org/10.1016/j.matpr.2020.08.232.
[25] K. Mahesh Babu, A. Ravitheja, Effect of copper slag as fine aggregate replacement in high strength concrete, Mater. Today Proc. 19 (2019) 409–414, https://doi.org/10.1016/j.matpr.2019.07.626.
[26] K.S. Al-Jabri, A.H. Al-Saidy, R. Taha, Effect of copper slag as a fine aggregate on the properties of cement mortars and concrete, Constr. Build. Mater. 25 (2011) 933–938, https://doi.org/10.1016/j.conbuildmat.2010.06.090.
[27] N. Gupta, R. Siddique, Strength and micro-structural properties of self-compacting concrete incorporating copper slag, Constr. Build. Mater. 224 (2019) 894–908, https://doi.org/10.1016/j.conbuildmat.2019.07.105.
[28] R. Sharma, R.A. Khan, Fresh and mechanical properties of self compacting concrete containing copper slag as fine aggregates, Constr. Build. Mater. 155 (2017) 617–629.
[29] F. Ameri, P. Shoaei, M. Zahedi, M. Karimzadeh, H.R. Musaeei, C.B. Cheah, Physico-mechanical properties and micromorphology of AAS mortars containing copper slag as fine aggregate at elevated temperature, J. Build. Eng. 39 (2021) 102289, https://doi.org/10.1016/j.jobe.2021.102289.
[30] K.S. Al-Jabri, M. Hisada, S.K. Al-Oraimi, A.H. Al-Saidy, Copper slag as sand replacement for high performance concrete, Cem. Concr. Compos. 31 (2009) 483–488, https://doi.org/10.1016/j.cemconcomp.2009.04.007.
[31] K.S. Al-Jabri, M. Hisada, A.H. Al-Saidy, S.K. Al-Oraimi, Performance of high strength concrete made with copper slag as a fine aggregate, Constr. Build. Mater. 23 (2009) 2132–2140, https://doi.org/10.1016/j.conbuildmat.2008.12.013.
[32] B. Patnaik, C. Bhojaraju, S.S. Mousavi, Experimental study on residual properties of thermally damaged steel fiber-reinforced concrete containing copper slag as fine aggregate, J. Mater. Cycles Waste Manag. 22 (2020) 801–815, https://doi.org/10.1007/s10163-020-00972-0.
[33] W. Gong, T. Ueda, Properties of self-compacting concrete containing copper slag aggregate after heating up to 400°C, Struct. Concr. 19 (2018) 1873–1880, https://doi.org/10.1002/suco.201700234.
[34] K. Ganesh Babu, V. Sree Rama Kumar, Efficiency of GGBS in concrete, Cem. Concr. Res. 30 (2000) 1031–1036, https://doi.org/10.1016/S0008-8846(00)00271-4.
[35] S. Kou, C. Poon, F. Agrela, Comparisons of natural and recycled aggregate concretes prepared with the addition of different mineral admixtures, Cem. Concr. Compos. 33 (2011) 788–795, https://doi.org/10.1016/j.cemconcomp.2011.05.009.
[36] S.C. Kou, C.S. Poon, M. Etxeberria, Residue strength, water absorption and pore size distributions of recycled aggregate concrete after exposure to elevated temperatures, Cem. Concr. Compos. 53 (2014) 73–82, https://doi.org/10.1016/j.cemconcomp.2014.06.001.
[37] T.M. Tung, O.E. Babalola, D. Le, Experimental investigation of the performance of ground granulated blast furnace slag blended recycled aggregate concrete exposed to elevated temperatures, Clean, Waste Syst. 4 (2023) 100069, https://doi.org/10.1016/j.clwas.2022.100069.
[38] A. Sahu, S. Kumar, A.K.L.S.S. Jeeva, Performance of recycled aggregate concrete incorporating copper slag at elevated temperature, Iran. J. Sci. Technol. Trans. Civ. Eng. (2024), https://doi.org/10.1007/s40996-024-01357-1.
[39] IS-12269:, Specification for 53 Grade Ordinary Portland Cement, Bur. Indian Stand., New Delhi,India, 1987. https://law.resource.org/pub/in/bis/S03/is.12269.b.1987.pdf.
[40] IS 16714 : 2018, Ground Granulated Blast Furnace Slag for Use of Cement, Mortar and Concrete -Specifications, 2018.
[41] M. Adams, A. Jayasuriya, Guideline Development for Use of Recycled Concrete Aggregates in New Concrete, vol. 18, ACI CRC, 2019, pp. 1–83, 517guide Lines, https://www.acifoundation.org/Portals/12/Files/PDFs/ACI_CRC_18-517_Final_report.pdf.
[42] IS:2386 Part 4, Methods of Test for Aggregates for Concrete: Mechanical Properties, BIS, 2016, pp. 1–37.
[43] BIS 383, Specification for Coarse and Fine Aggregates from Natural Sources for Concrete, Bur. Indian Stand., Delhi, 2016, pp. 1–24.
[44] IS:2386- Part I, Method of Test for Aggregate for Concrete. Part I - Particle Size and Shape, Indian Stand., 1963 (Reaffirmed 2002).
[45] IS 10262, Concrete Mix Proportioning- Guidelines, Bur. Indian Stand. Second Rev (2019) 1–40.
[46] M.H. Lai, Z.Y. Lu, Y.T. Luo, F.M. Ren, J. Cui, Z.R. Wu, J.C.M. Ho, Pre- and Post-fire Behaviour of Glass Concrete from Wet Packing Density Perspective, vol. 86, 2024, https://doi.org/10.1016/j.jobe.2024.108758.
[47] M.H. Lai, Z.H. Chen, J. Cui, J.P. Zhong, Z.R. Wu, J.C.M. Ho, Enhancing the post-fire behavior of steel slag normal-strength concrete by adding SCM, Constr. Build. Mater. 398 (2023), https://doi.org/10.1016/j.conbuildmat.2023.132336.
[48] M.H. Lai, Y.M. Xie, B.X. Zhang, F.M. Ren, S. Kitipornchai, J.C.M. Ho, Iron sand heavy-weight concrete – pre- and post-fire characteristics from wet packing density perspective, Constr. Build. Mater. 435 (2024), https://doi.org/10.1016/j.conbuildmat.2024.136728.
[49] IS 516 (Part 1/Sec 1) : 2021, Hardened Concrete - Methods of Test, Bur. Indian Stand. First Revi, 2021, pp. 1–20. www.standardsbis.in.
[50] IS 516 (Part 8/Sec 1) : 2020, Hardened Concrete- Methods of Test, vol. 516, Bur. Indian Stand., 2020.
[51] IS:7320-1974, Specification for Concrete Slump Test Apparatus, Indian Stand, 1974.
[52] M.H. Lai, Z.C. Huang, C.T. Wang, Y.H. Wang, L.J. Chen, J.C.M. Ho, Effect of fillers on the behaviour of low carbon footprint concrete at and after exposure to elevated temperatures, J. Build. Eng. 51 (2022) 104117, https://doi.org/10.1016/j.jobe.2022.104117.
[53] Z.C. Huang, J.C.M. Ho, J. Cui, F.M. Ren, X. Cheng, M.H. Lai, Improving the post-fire behaviour of steel slag coarse aggregate concrete by adding GGBFS, J. Build. Eng. 76 (2023) 107283, https://doi.org/10.1016/j.jobe.2023.107283.
[54] Z. Huang, B. Zhang, J.C.M. Ho, F. Ren, M. Lai, Improving passing ability of ultra-heavy-weight concrete by optimising its packing structure, Mag. Concr. Res. 76 (2024) 1266–1278, https://doi.org/10.1680/jmacr.24.00143.
[55] H. Zhao, F. Liu, H. Yang, Residual compressive response of concrete produced with both coarse and fine recycled concrete aggregates after thermal exposure, Constr. Build. Mater. 244 (2020) 118397, https://doi.org/10.1016/j.conbuildmat.2020.118397.
[56] R.K. Majhi, A.N. Nayak, Bond, durability and microstructural characteristics of ground granulated blast furnace slag based recycled aggregate concrete, Constr. Build. Mater. 212 (2019) 578–595, https://doi.org/10.1016/j.conbuildmat.2019.04.017.
[57] E.D. Shumuye, J. Zhao, Z. Wang, Effect of the curing condition and high-temperature exposure on ground-granulated blast-furnace slag cement concrete, Int. J. Concr. Struct. Mater. 15 (2021), https://doi.org/10.1186/s40069-020-00437-6.
[58] C.J. Zega, A.A. Di Maio, Recycled concrete exposed to high temperatures, Mag. Concr. Res. 58 (2006) 675–682, https://doi.org/10.1680/macr.2006.58.10.675.
[59] S. Aydin, Development of a high-temperature-resistant mortar by using slag and pumice, Fire Saf. J. 43 (2008) 610–617, https://doi.org/10.1016/j.firesaf.2008.02.001.
[60] G.F. Peng, Z.S. Huang, Change in microstructure of hardened cement paste subjected to elevated temperatures, Constr. Build. Mater. 22 (2008) 593–599, https://doi.org/10.1016/j.conbuildmat.2006.11.002.